

## Supplementary Materials:

### Experimental Evidence for a Two-Stage Freezing Process in Colloidal Crystallites

J.R. Savage and A.D. Dinsmore

*Department of Physics, University of Massachusetts, Amherst MA 01003*

Figure S1 shows snapshots of four samples soon after heating, before persistent crystalline clusters appeared. For clarity, the images shown are  $250 \times 250$  pixels, smaller than the full-frame size of  $640 \times 486$  pixels. These snapshots were taken soon after raising  $T$  to the steady-state level (which actually corresponds to supercooling, since depletion becomes stronger with increasing  $T$ ). In all cases, a background of amorphous clusters is seen. Particles in these clusters have liquid-like mobility. The ordered crystallite seen in the upper-right quadrant of (a) vanished within a few seconds; it appears to have been smaller than the critical size. In (b-d), crystallites grew from the amorphous clusters once they reached a size of  $\sim 20$ -30 (see main text for details). In (a,b,d), the amorphous clusters were metastable with respect to the gas and eventually broke up (except for a very few that crystallized and grew). Hence the average cluster size was nearly constant (Fig. S2). For the sample of Fig. S1(c), the average cluster size grew continuously (Fig. S2).

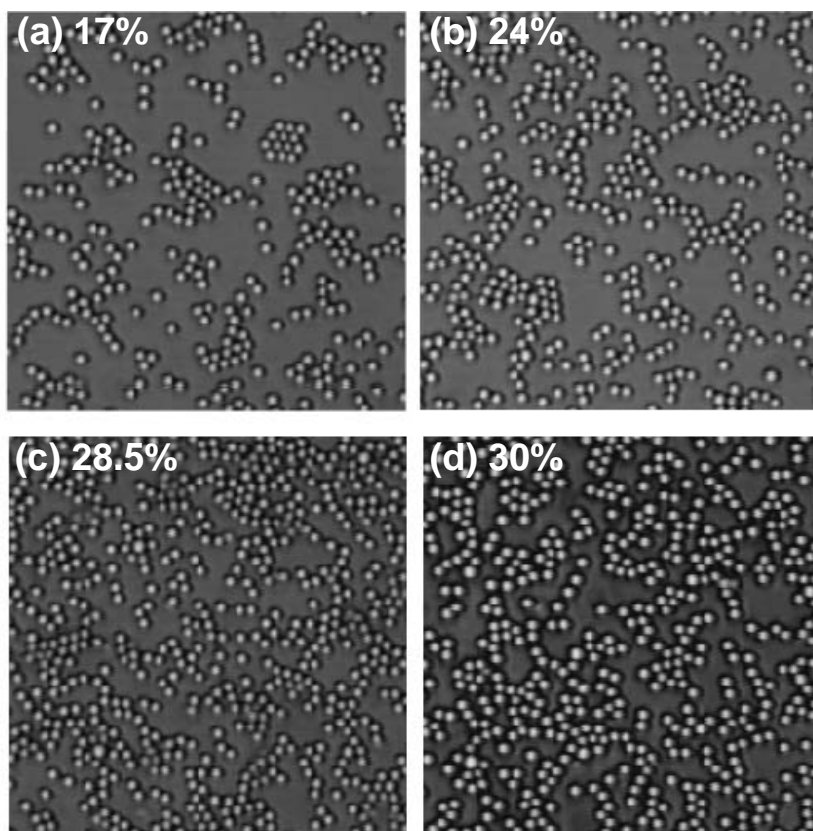


FIG. S1. Images in (a-d) have area fractions  $\eta = 17\%$ ,  $24\%$ ,  $28.5\%$  and  $30\%$ , respectively.

Figure S2 shows the sample-average cluster size  $\langle N \rangle$  as a function of time  $t$ . We considered only clusters with  $N > 6$  because the smaller clusters were very numerous and dominated the statistics. There is a clear distinction between samples where  $\langle N \rangle$  remained nearly constant and those where  $\langle N \rangle$  grew (*i.e.*, the 28.5% and 34% samples, which were at the relatively high temperatures (deep supercooling) of 35 °C and 30 °C, respectively). We concluded that the latter two samples lay within the metastable gas-liquid coexistence region. This conclusion is further supported by their having lower chemical potential in the fluid than gas (*i.e.*,  $\Delta\mu < 0$ ; see Fig. S3 and text).

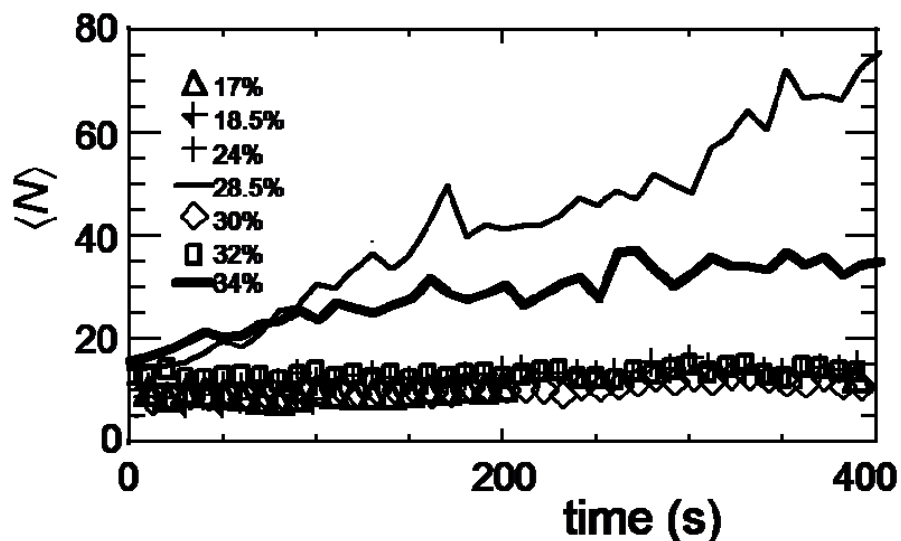


FIG. S2. Plot of the measured average cluster size,  $\langle N \rangle$ , as a function of time for seven samples with different area fractions  $\eta$ . This analysis considers only clusters with  $N > 6$ .

Figure S3 shows the plots of  $-\ln(n_N/n_1)$ , where  $n_N$  is the number of clusters of size  $N$  and  $n_1$  is the number of spheres (monomers;  $N = 1$ ). These plots show only the data for the first 100 s. During this time, the 17% and 30% samples had no stable crystallites. For these samples, the cluster-size distribution appeared stationary in time, and we interpret  $-\ln(n_N/n_1)$  as the free energy cost of a cluster of size  $N$  relative to that of a monomer. The lines show the best-fit to the form  $(\Delta\mu)N + (\eta_c^{1/2}\pi\Gamma)N^{1/2}$ , where  $\Delta\mu$  is the fitted chemical potential of these clusters (which are amorphous) minus that of the gas. The second term represents the interfacial energy;  $\Gamma$  is the line tension in units of  $k_B T$  per sphere diameter and  $\eta_c$  is the area fraction of the cluster. For numerical simplicity, we assume clusters were circular and set  $\eta_c = (3/\pi)^2 = 0.91$ . (Recent molecular dynamics simulations of freezing in 3D with Lennard-Jones interactions show that nucleating crystallites might not be spherical [S1]; we will investigate this point later.)

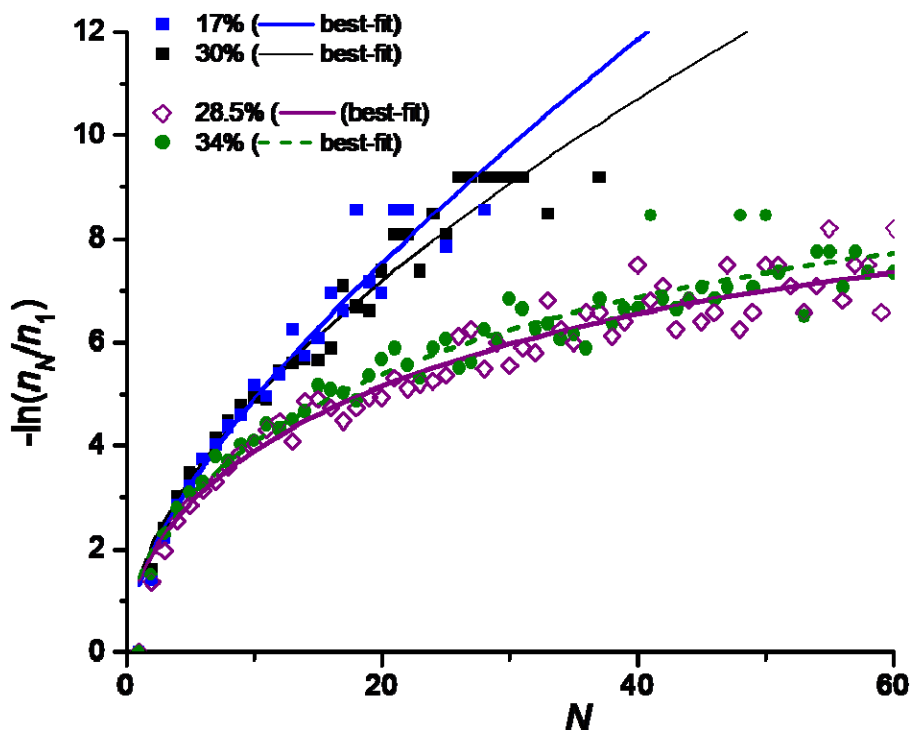


FIG. S3. A plot of measured  $-\ln(n_N/n_1)$  vs  $N$ , where  $n_N$  is the number of clusters of size  $N$ . Data for the first 100 s of video is shown; in the 17% and 30% samples, there were no stable crystallites during this time. The fit is to a simple nucleation-like model,  $aN + b\sqrt{N}$ , where the second term indicates the interfacial energy of a cluster. The lines show the best-fit results. The numerical results are given in the main text.

Figure S4 shows the crystalline order just for particles with  $Z < 6$ . Following our earlier convention [S2], for each cluster we first find all particles  $j$  for which  $Z_j < 6$ . We then calculate  $C_6(j) \equiv \langle |(1/Z_j) \sum_k \psi_6(j) \psi_6^*(k)|^2 \rangle$ , where  $\sum_k$  refers to a sum over all neighbors ( $k$ ) of  $j$  regardless of  $Z_k$ . As was reported in the context of sublimation, the sudden onset of order for the sample with are fraction  $\eta = 30\%$  at  $N \approx 25$  shows that the ordering occurs for all particles, not just for the ‘core’ particles having  $Z = 6$ .

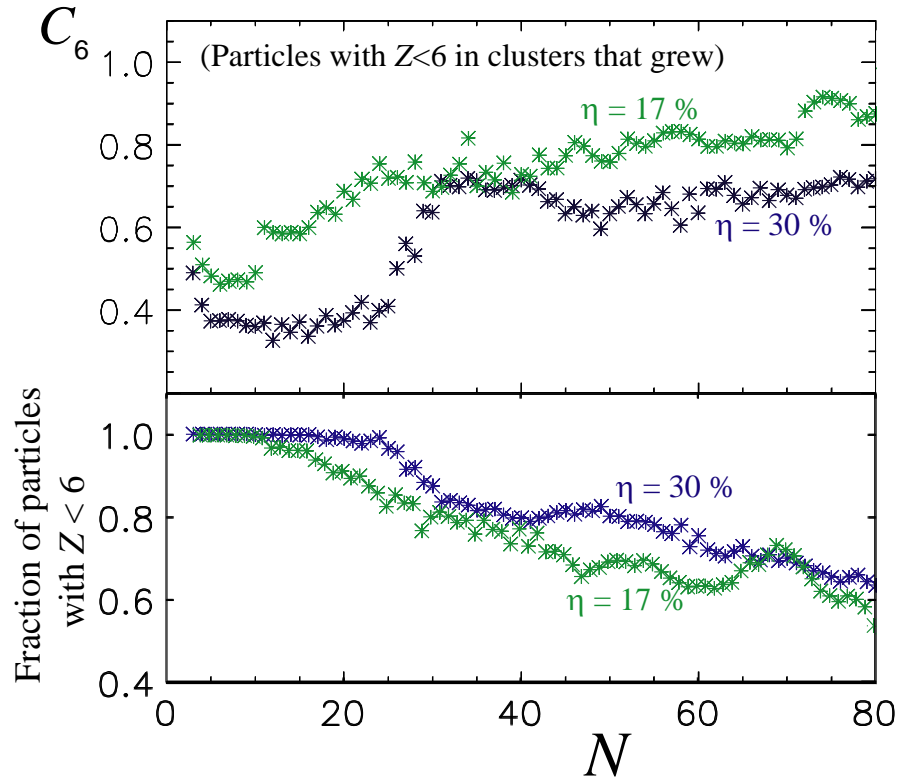


FIG. S4. Plot of the average value of  $C_6$  for all particles having fewer than 6 bonds ( $Z < 6$ ). For the 30% sample that showed two-step nucleation, these ‘perimeter’-like particles also underwent an onset of order at  $N$  approximately 25. The two-step behavior is much less evident in the sample with  $\eta = 17\%$ , as reported in the main text.

### References:

- [S1] F. Trudu, D. Donadio, and M. Parrinello, Phys. Rev. Lett. **97**, 105701 (2006).  
[S2] J. R. Savage, *et al.*, Science **314**, 795 (2006).